

## Time-resolved, in situ DRIFTS/EDE/MS studies on alumina supported Rh catalysts: effects of ceriation on the Rh catalysts in the process of CO oxidation

Anna B. Kroner, Mark A. Newton, Moniek Tromp, Andrea E. Russell, Andrew J. Dent & John Evans

To cite this article: Anna B. Kroner, Mark A. Newton, Moniek Tromp, Andrea E. Russell, Andrew J. Dent & John Evans (2017) Time-resolved, in situ DRIFTS/EDE/MS studies on alumina supported Rh catalysts: effects of ceriation on the Rh catalysts in the process of CO oxidation, *Catalysis, Structure & Reactivity*, 3:1-2, 13-23, DOI: [10.1080/2055074X.2016.1266762](https://doi.org/10.1080/2055074X.2016.1266762)

To link to this article: <http://dx.doi.org/10.1080/2055074X.2016.1266762>



© 2017 The Author(s). Published by Informa UK Limited, trading as Taylor & Francis Group



[View supplementary material](#)



Published online: 14 Feb 2017.



[Submit your article to this journal](#)



Article views: 32




[View related articles](#)



[View Crossmark data](#)

## Time-resolved, *in situ* DRIFTS/EDE/MS studies on alumina supported Rh catalysts: effects of ceriation on the Rh catalysts in the process of CO oxidation

Anna B. Kroner<sup>a,d</sup>, Mark A. Newton<sup>b</sup>, Moniek Tromp<sup>c,d</sup>, Andrea E. Russell<sup>d</sup>, Andrew J. Dent<sup>a</sup> and John Evans<sup>a,d,e</sup> 

<sup>a</sup>Diamond Light Source, Chilton, UK; <sup>b</sup>Department of Physics, University of Warwick, Coventry, UK; <sup>c</sup>Faculty of Science, Van't Hoff Institute for Molecular Sciences, University of Amsterdam, Amsterdam, Netherlands; <sup>d</sup>School of Chemistry, University of Southampton, Southampton, UK; <sup>e</sup>Rutherford Appleton Laboratory, Research Complex at Harwell, Didcot, UK

### ABSTRACT

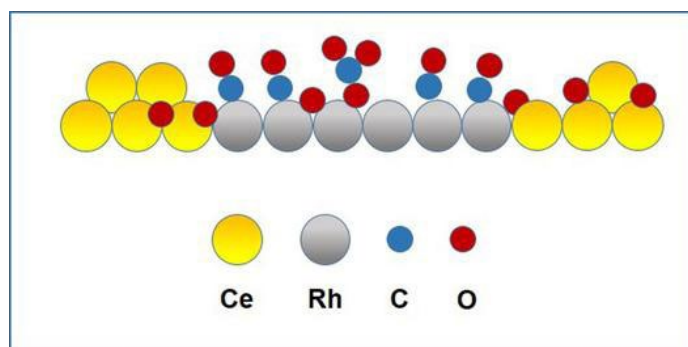
The effect of ceria doping by oxide surface modification and controlled metal surface modification (CSM) on the structure-function properties of Rh/ $\gamma$ -Al<sub>2</sub>O<sub>3</sub> catalysts in the process of CO oxidation were studied by a combined array of Diffuse Reflectance Infrared Fourier Transform Spectroscopy (DRIFTS)/Energy Dispersive X-ray Absorption Fine Structure/Mass Spectrometry techniques applied simultaneously under time-resolved, *in situ* conditions in the temperature range of 298–573 K. The addition of each promoter element by CSM exhibits multiple effects on the catalysts structure. The DRIFTS/XAS studies indicate that CeO<sub>x</sub> facilitate the protection of Rh particles against extensive oxidation in atmospheres of air, O<sub>2</sub> and CO, without reducing the coverage of oxidisable adsorbed CO.

### ARTICLE HISTORY

Received 27 September 2016  
Accepted 25 November 2016

### KEYWORDS

DRIFTS; XAS; Rh catalyst; CO oxidation; ceria




### Introduction

The process of CO oxidation over Rh catalysts has been a subject of many experimental investigations [1–6] due to its industrial and environmental importance of removing CO from chemical processes and automotive exhausts [7–9], and traces of CO from H<sub>2</sub> feed gas for fuel cells [10,11]. It has been widely reported that the process of CO oxidation is promoted by incorporation of CeO<sub>x</sub> oxides with Rh nanoparticles supported on alumina [12,13]; oxidation and reduction of ceria are fast allowing oxygen storage during O<sub>2</sub> rich periods and release during O<sub>2</sub> lean periods through transfer of lattice oxygen from bulk to surface [13]. An intimate contact between the CeO<sub>2</sub> based oxides and Rh metal may alter the oxidation state of the supported Rh particles and it has been concluded that two Rh types of surface sites

(zero-valent and oxidised) may explain the striking differences observed in CO–O<sub>2</sub> kinetics on CeO<sub>2</sub>-promoted Rh catalysts compared with undoped versions [14].

This study is focussed on 4 wt% Rh-based materials supported on  $\gamma$ -Al<sub>2</sub>O<sub>3</sub> and doped with CeO<sub>x</sub> prepared from  $\beta$ -diketonate metallo-organic precursor to about a stoichiometric level with regard to Rh. We have reported that, either by oxide surface modification (OSM) of the alumina, or by controlled surface modification (CSM) of the pre-formed rhodium particles, a close proximity of these elements on the alumina surface was confirmed by EDX measurement [15]; in contrast, segregation was observed more with conventional methods using inorganic sources. TEM results of Rh catalysts published in our previous paper have shown relatively narrow particle size distributions with Rh particles ranging from

**CONTACT** Anna B. Kroner  [anna.kroner@diamond.ac.uk](mailto:anna.kroner@diamond.ac.uk)

 Supplemental data for this article can be accessed <http://dx.doi.org/10.1080/2055074X.2016.1266762>

© 2017 The Author(s). Published by Informa UK Limited, trading as Taylor & Francis Group.

This is an Open Access article distributed under the terms of the Creative Commons Attribution License (<http://creativecommons.org/licenses/by/4.0/>), which permits unrestricted use, distribution, and reproduction in any medium, provided the original work is properly cited.

approximately 0.7–4 nm [15]. There is a clear shift to a lower Rh particle size distribution for the ceriated Rh catalysts (OSM). On another hand, the ceriated Rh catalysts (CSM) show clearly a larger mean particle size. When studying the CO chemisorption on a series of Rh catalysts by a combined array of XAS/diffuse reflectance infrared Fourier transform spectroscopy (DRIFTS)/mass spectrometry (MS) in the lower temperature regime (323–423 K) geminal dicarbonyl species adsorbed on Rh are dominant entities formed on the surface of unpromoted Rh/Al<sub>2</sub>O<sub>3</sub> and Rh/CeO<sub>x</sub>/Al<sub>2</sub>O<sub>3</sub> (OSM) while the EXAFS analysis suggests reduction of Rh particle size and elongation of RhRh bonds [16]. In contrary, only for the Rh/CeO<sub>x</sub>/Al<sub>2</sub>O<sub>3</sub> (CSM) catalysts, CO was found to mainly be adsorbed as linear and bridged species on the surface of supported Rh.

Therefore, the emphasis of this paper is to examine the effect of the heterometal such as Ce on the behaviour of Rh/Al<sub>2</sub>O<sub>3</sub> during the reaction with CO and O<sub>2</sub> by investigations of the structure-function relationships of these catalysts *in situ* by the combined techniques of energy dispersive extended X-ray absorption fine structure (EDE), DRIFTS and MS.

## Results and discussion

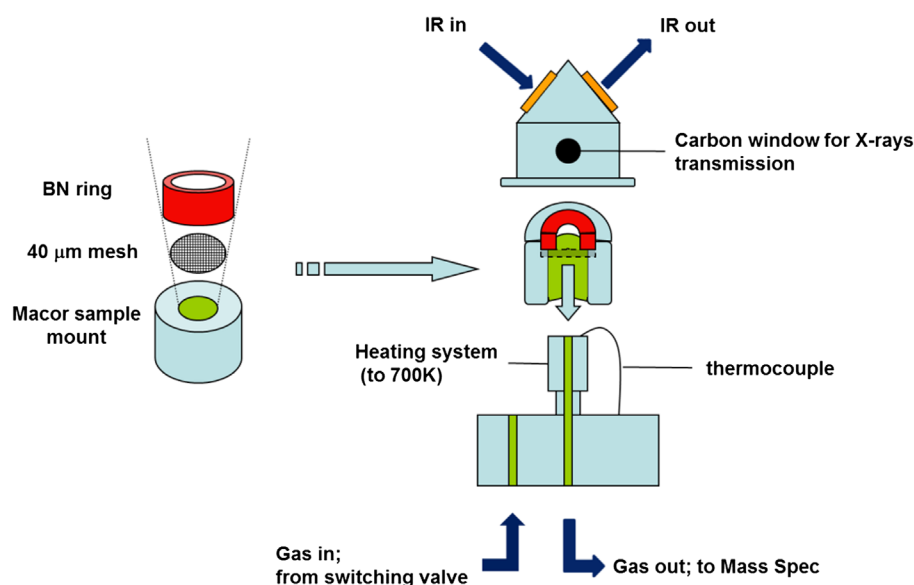
### Experimental procedures

The process of CO oxidation over a series of Rh catalysts was studied applying the O<sub>2</sub>/CO gas switching in the DRIFTS cell by combined EDE/DRIFTS/MS apparatus. Figure 1 shows the reaction cell compatible for DRIFTS/EDE experiments. The X-ray path is directed through a small catalytic cell, perpendicular to the IR beam direction. A sample cup is made from boron nitride to permit transmission of X-rays through the sample. The reaction cell set up allows gas switching under a constant gas

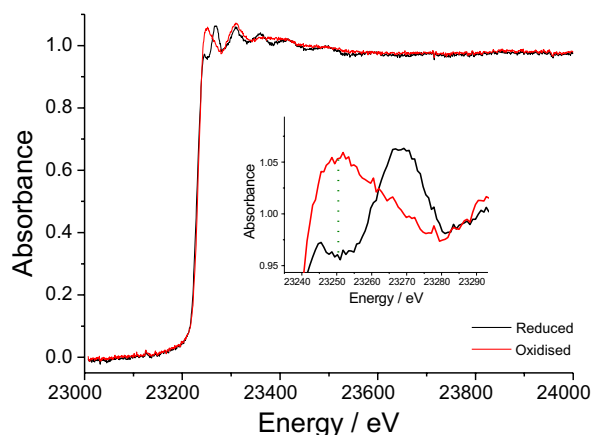
flow of 25 mlmin<sup>-1</sup> and sample heating up to 700 K. The whole sample environment is mounted on an optical bench besides the DRIFTS spectrometer with a high sensitivity MCT detector of IR beam. Mass spectrometer is directly connected to the cell via a capillary.

Prior to the experiment, the catalyst was pre-treated *in situ* by heating up to 573 K under a flow of 5% H<sub>2</sub>/He, and then oxidising the sample under 5% O<sub>2</sub>/He until the H<sub>2</sub>O and any carbonaceous deposition was not-detectable from the system (by MS). Finally the sample was reduced again under 5% H<sub>2</sub>/He. After the full pre-treatment, the system was cooled down in H<sub>2</sub> to the working temperature and purged by He. O<sub>2</sub>/CO switching experiments were performed over a series of Rh catalysts at selected temperatures: 323, 373, 423, 473 and 573 K using a mixture of 5% O<sub>2</sub>/He and 5% CO/He, respectively. The O<sub>2</sub>/CO switching experiment was studied over the Rh catalysts at two different times of gas exposure: 20 s at 473–573 K and 45 s in the lower temperature range of RT–423 K.

The O<sub>2</sub>/CO switching experiment was initially examined for each Rh catalyst by following the X-ray absorption near edge structure (XANES) variations. Figure 2 shows the normalised Rh K-edge EDE data taken at 573 K for both reduced and oxidised 4 wt% Rh/Al<sub>2</sub>O<sub>3</sub> with an acquisition time of 100 ms. The energy of 23246 eV, highlighted by a green dashed line, shows maximal changes in absorbance ( $\Delta$ XANES = difference between absorbance of fully oxidised and fully reduced Rh) so that approximation was used for speciation. The presence of metallic Rh species during the CO exposure step can be also confirmed by DRIFTS, shown in Figure S1, where linear and bridging species are formed. In addition, we can also observe a significant contribution from rhodium gem-dicarbonyl species [RhO<sup>I</sup>(CO)<sub>2</sub>], which was also considered for the  $\Delta$ XANES calculation.



**Figure 1.** The cross-section of the XAFS/DRIFTS cell.



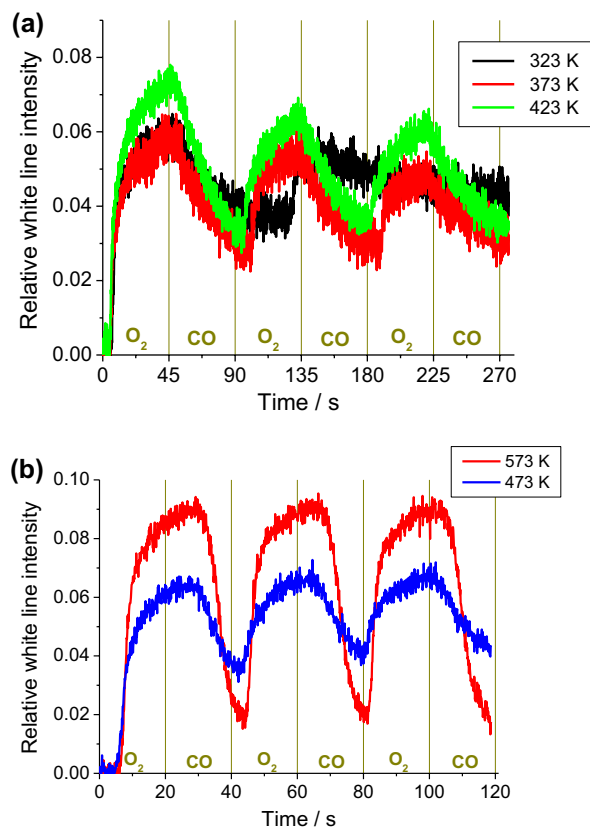
**Figure 2.** Normalised EDE absorption data derived from fully reduced (black line) and oxidised (red line) 4 wt% Rh/Al<sub>2</sub>O<sub>3</sub> at 573 K. The green dashed line highlights the energy in XANES that is used to follow the redox cycles.

Figure S2 presents the Rh K-edge XANES of Rh(0), Rh<sub>2</sub>O<sub>3</sub> and RhO(CO)<sub>2</sub> collected on BM29 in the scanning mode. As expected, the absorption edge shifts towards higher energy with the increasing Rh oxidation state. However, looking at the energy of 23246 eV, the white line intensities between Rh(0) and Rh(+) are very similar and considering that XANES data collected in the EDE mode have much lower signal-to-noise ratio, it would be very difficult to discriminate the differences between Rh(+) and Rh(0) contributions of the studied materials looking only at the white line intensity of the EDE data. Therefore, the presented variation in the white line intensity is an approximate representation of the oxidised and the reduced forms and an error of 10% needs to be considered when interpreting the data.

### Behaviour of Rh/Al<sub>2</sub>O<sub>3</sub> under O<sub>2</sub> and CO

The dynamic response of 4 wt% Rh/Al<sub>2</sub>O<sub>3</sub> to oxidation and then reduction by CO as a function of time at a given temperature was monitored by Rh K-edge XANES at 23246 eV (Figure 3). During oxygen exposure the variations of white line intensity increases (oxidised rhodium) and while under CO the rhodium is more reduced. The variation of the XANES indicates an increase in Rh oxidation with temperature. The level of Rh oxidation at 323 and 373 K after the first O<sub>2</sub> switch is equivalent. At 323 K the rhodium particles are increasingly oxidised during the second cycle; the last cycle (O<sub>2</sub>/CO) does not modify the Rh oxidation state. In the range of temperatures, 373–423 K, the repeated cycles (O<sub>2</sub>/CO) cause a progressive decrease in the degree of oxidation of the Rh. The white line intensity variations at higher temperature 473–573 K show increasing oscillations for each cycle.

An overview of IR active species observed on 4 wt% Rh/Al<sub>2</sub>O<sub>3</sub> during CO exposure of the first, second and third cycle at the temperature range of 323–573 K is shown in Figure S1. At 323 K, the IR spectrum displays the two sharp peaks at 2101 and 2029 cm<sup>-1</sup> assigned



**Figure 3.** Changes in Rh K-edge XANES at 23246 eV of 4 wt% Rh/Al<sub>2</sub>O<sub>3</sub> starting from the reduced catalyst monitored during O<sub>2</sub> and CO exposure at (a) 323, 373, 423, and (b) 473 and 573 K. The catalyst was exposed to 5% O<sub>2</sub>/He at 473 and 573 K at the switching times of 0–20 s (I cycle), 40–60 s (II cycle), 80–100 s (III cycle), the flowing gas was switched to CO/He at the switching times of 20–40 s (I cycle), 60–80 s (II cycle) and 100–120 s (III cycle). At lower temperature regime, below 473 K, the catalyst was exposed to 5% O<sub>2</sub>/He at the switching times of 0–45 s (I cycle), 90–135 s (II cycle), 180–225 s (III cycle), the flowing gas was switched to CO/He at the switching times of 45–90 s (I cycle), 135–180 s (II cycle) and 225–270 s (III cycle). Delays are evident between the switching time and the X-ray response, probably due to diffusion delays.

respectively to the symmetric and asymmetric rhodium(I) geminal dicarbonyl species, Rh<sup>I</sup>(CO)<sub>2</sub>. These bands are overlapped with the signal of the linear Rh–CO on Rh metal at 2071 cm<sup>-1</sup>. A broad band present around 1880 cm<sup>-1</sup> is ascribed to bridged CO. Additionally, a new band appears at ca. 2126 cm<sup>-1</sup> which is assigned to a RhO(CO) species with a higher Rh oxidation state [17]. This speciation is consistent with previous reports [18,19]. At 423–473 K the O<sub>2</sub>/CO switches decrease the proportion of linear and bridged CO species, keeping the evolution of geminal dicarbonyl species constant, and at 573 K, only IR bands of the CO on metallic rhodium are observed.

Furthermore, a bathochromic shift is observed for the linear CO species when increasing the temperature, from  $\nu \sim 2071$  cm<sup>-1</sup> at 323 K to  $\nu \sim 2062$  cm<sup>-1</sup> at 473 K, and to  $\nu \sim 2043$  cm<sup>-1</sup> at 573 K. This shift is consistent with the lower CO coverage due to a change in electron density of particles and reduction in the inter-CO

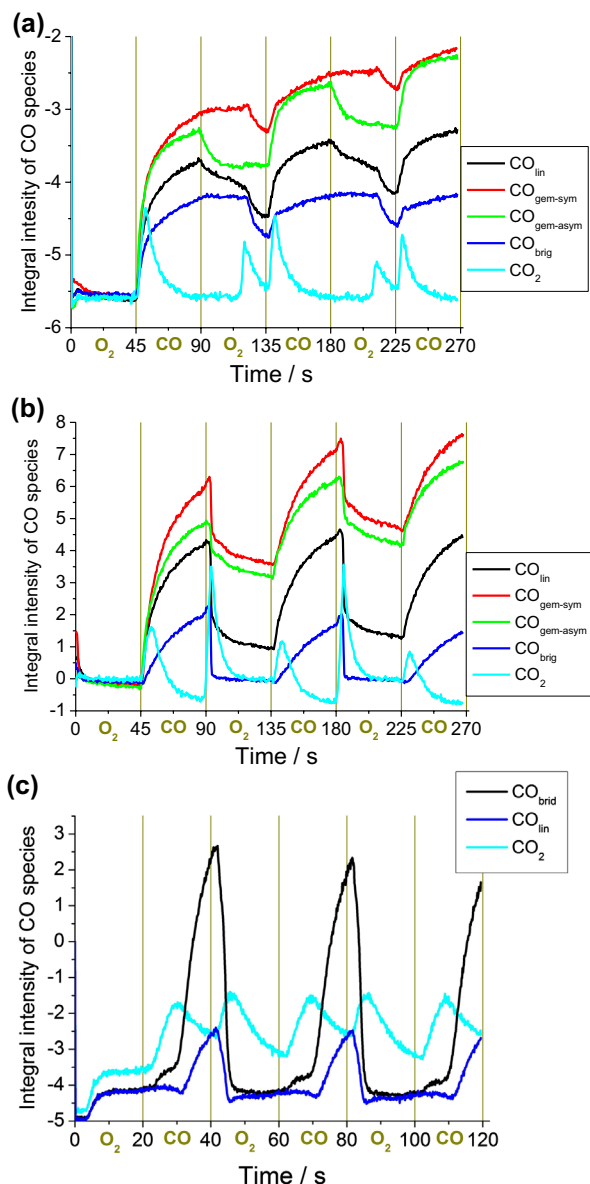


**Figure 4.** Variation of integral intensity of CO species adsorbed on the Rh surface during the  $O_2$ /CO switching experiment over 4 wt% Rh/ $Al_2O_3$  at (a) 323 K, (b) 423 K, (c) 573 K. The intensities of the IR bands at the energies of the symmetric and asymmetric bands of  $Rh(CO)_2$  are shown in green and red, respectively. The catalyst was exposed to 5%  $O_2$ /He at the switching times of 0–20 s (I cycle), 40–60 s (II cycle), 80–100 s (III cycle), the flowing gas was switched to CO/He at the switching times of 20–40 s (I cycle), 60–80 s (II cycle) and 100–120 s (III cycle).

vibrational coupling as described in the pioneering work of Yang and Garland [19]. As the studied Rh catalysts exhibit similar behaviour as detected by IR upon  $O_2$ /CO switches at the range of temperatures, 323–473 K for Rh/ $Al_2O_3$ , only an analysis of the experiments done at 323, 423 and 573 K is described in this paper.

The evolution of  $Rh^I(CO)_2$ , linear and bridged CO species adsorbed on the Rh surface and the formation of  $CO_2$  in the gas phase as a function of time through the gas switching cycles is shown in Figure 4 (The integral intensity of the symmetric  $\nu(CO)$  mode of  $Rh^I(CO)_2$  includes an overlapping contribution to the evolution of gas phase CO). At 323 K following the second cycle

partial loss of these species occurs at the expense of some  $CO_2$  production. In the next CO/ $O_2$  switches the proportion of  $Rh^I(CO)_2$  increases, indicating that more  $Rh(+)$  species are present in studied catalysts and the subsequent  $O_2$  exposures cause further structural disruption of Rh particles. Interestingly, we observed that the evolution of band assigned to the symmetric mode of the Rh geminal dicarbonyl species (red line) under  $O_2$  exposure (II and III cycle) progressed until the last few seconds of  $O_2$  switch, unlike the asymmetric mode. That could indicate that another CO species adsorbed on Rh surface whose IR frequency is in a region of  $2100\text{ cm}^{-1}$ . This unknown carbonyl site displayed a different kinetic profile. Consistent with this the pioneering work of Yates et al. [20], describing the IR studies on CO chemisorbed on Rh/ $Al_2O_3$  under cryogenic conditions, indicated that a higher apparent intensity of the symmetric  $Rh^I(CO)_2$  mode was observed at temperatures below 173 K. At 423 K, the extent of the CO desorption increased, but both symmetric and asymmetric  $Rh^I(CO)_2$  intensities follow each other consistently indicating this species is predominant at that temperature. At 573 K the Rh structure is substantially different, there being no  $Rh^I(CO)_2$  bands. The linear and bridged CO species show clear oscillations of their concentrations during CO exposure and through the oxidising step producing  $CO_2$  gas. The integration of the bridging CO species diminished gradually through the ensuing cycles.

The combined XANES/DRIFTS studies (Figure S3 for 573 K run) for 4 wt% Rh/ $Al_2O_3$  display good correlations between the techniques. After 10 s of CO exposure the degree of Rh oxidation significantly decreases and simultaneously the linear and bridged CO species develops on the Rh surface. Following  $O_2$  exposure in the second cycle, the CO species adsorbed are rapidly converted to  $CO_2$ . After complete removal of CO from the metallic surface the Rh particles are oxidised to a similar extent as in the first cycle. During the third ( $O_2$ /CO) cycle similar behaviour of the Rh particles is observed. A delay of 10 s is due to the fact that gas needed to go through a whole sample bed from the bottom to the top part of the packed bed where the X-ray beam is focused. The X-ray beam position close to the surface of the catalysts bed is aligned well with the IR beam position that gives the most representative catalysts area measured by the synchronised multiple technique approach.

Figure 5 shows the mass spectrometric responses for  $O_2$ , CO,  $CO_2$  obtained for 4 wt% Rh/ $Al_2O_3$  during  $O_2$ /CO switches at 573 K (cycle times of 40 s). In all Rh systems, the formation of  $CO_2$  gas occurs after each gas change, consistent with previous findings [21,22].

By analysing the EXAFS data at the beginning and at the end of each  $O_2$ /CO step of the time-resolved experiment, structural parameters of Rh particles studied at 573 K are reported in Table 1 and  $k^3$ -weighted Rh K-edge EXAFS and FT fittings are presented in Figure 6(a) and (b).

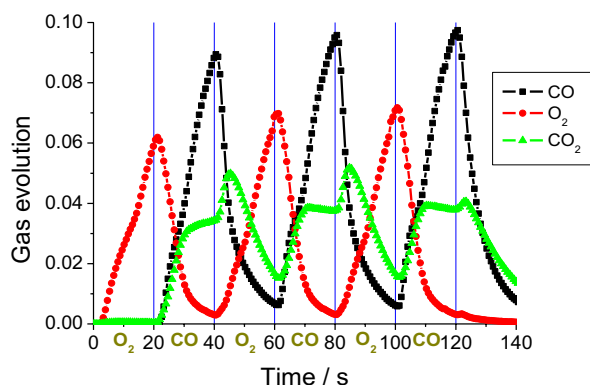


**Figure 5.** Evolution of reactants (CO and O<sub>2</sub>) and product (CO<sub>2</sub>) over 4 wt% Rh/Al<sub>2</sub>O<sub>3</sub> upon reaction at 573 K during O<sub>2</sub>/CO switching experiment.

**Table 1.** Structural and statistical parameters derived from the analysis of Rh K edge EXAFS over 4 wt% Rh/Al<sub>2</sub>O<sub>3</sub> at O<sub>2</sub>/CO atmosphere at 573 K. Data range used was 3–11 Å<sup>-1</sup>. *R* fitting range 1–6 Å. AFAC = 1. Values in parenthesis are statistical errors generated in EXCURV98.

Conditions	Scatterer	CN	<i>r</i> /Å <sup>a</sup>	DW/Å <sup>b</sup>	<i>R</i> /%
He–step I	Rh	5.7 (3)	2.64 (1)	0.0175	39
5%O <sub>2</sub> /He	Rh	1.3 (2)	2.66 (1)	0.0175	47
–step II	O	2.6 (2)	2.04 (1)	0.0180	
5%CO/He	Rh	4.3 (2)	2.64 (1)	0.0175	45
–step III	O	1.0 (3)	2.09 (3)	0.018	
	C	1.0 (1)	1.92 (2)	0.022	
	O	1.0 (1)	2.93 (2)	0.023	

<sup>a</sup>Coordination number

<sup>b</sup>Debye Waller factor =  $2\sigma^2$ .

For the oxidised Rh phase, only a short *k*-range of EXAFS data, between 3 and 9 k, displayed clear oscillatory character, this being significantly muted beyond 6 k due to the light scattering neighbouring atoms of oxygen surrounding Rh absorber.

The variations in the Rh–Rh coordination number during the O<sub>2</sub>/CO switching experiment over 4 wt% Rh/Al<sub>2</sub>O<sub>3</sub> in the temperature range of 373–573 K (Figure 7) show substantial changes of the Rh particle size. The static EDE data at 573 K on the pre-reduced catalyst affords a CN<sub>Rh–Rh</sub> of ca. 5.7. Upon exposure to a flow of 5% O<sub>2</sub>/He for 20 s, the EXAFS curve indicates significant structural changes that induced a rapid oxidation, with the coordination number of RhRh shell falling to a value of ca. 1.3. Assuming a constant spherical morphology and fcc structure [23], these CN<sub>RhRh</sub> values correspond to an average particle with ca. 13–21 Rh atoms reducing to particles of ca. 2–4 Rh atoms, respectively. The RhRh occupation subsequently increases during CO exposure. The CN<sub>RhRh</sub> variations between the oxidised and metallic form of Rh catalyst during the O<sub>2</sub>/CO cycles appear to be smaller at lower temperature range. The presence of an additional RhO shell at 2.04 Å with the RhO coordination number of ca. 2.6 clearly shows the predominantly oxidised state of the Rh. These results are consistent with the scanning EXAFS results reported by Martens et al. [24,25] The structure of the Rh catalysts present

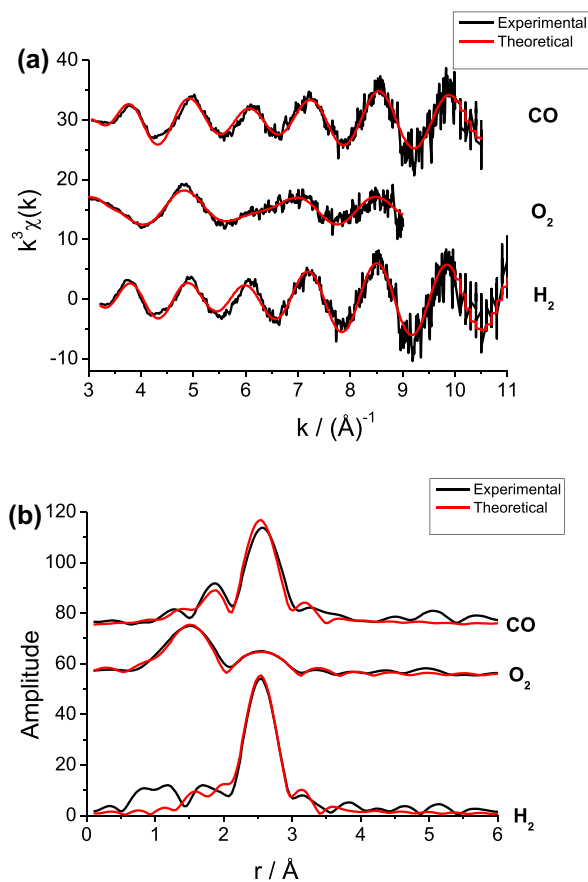


**Figure 6.** (a) *k*<sup>3</sup> weighted Rh EDE data and (b) the Fourier transforms (corrected on Rh scatterer) derived from the analysis done over 4 wt% Rh/Al<sub>2</sub>O<sub>3</sub> under 5% H<sub>2</sub>/He, 5% O<sub>2</sub>/He and 5% CO/He at 573 K. Analysis on ten averaged experimental spectra.

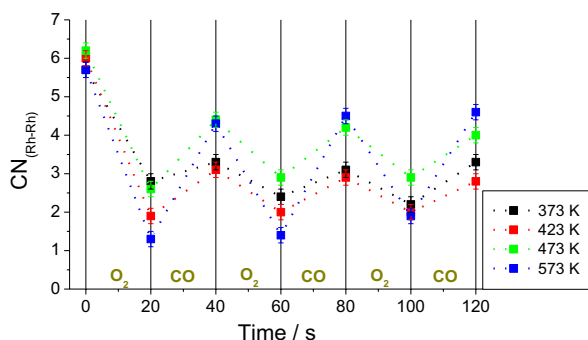


**Figure 7.** Variations of RhRh coordination number during the O<sub>2</sub>/CO switching experiment over 4 wt% Rh/Al<sub>2</sub>O<sub>3</sub> at the temperature indicated.

upon O<sub>2</sub> exposure at 573 K has been compared with the crystal structure of Rh oxides and the Rh surface oxide based on the Fourier transform calculations [15]. Controlled oxidation carried out over a thin surface of Rh(111) [26] and Rh(110) [27] indicated the formation of a hexagonal trilayer of O–Rh–O on the surface of the metal. An initial oxidation of Rh nanoparticles which forms a thin layer of oxide surrounding the metallic core can be viewed as a facile process as already observed for 5 wt% Rh catalysts [4]. However, any subsequent oxidation becomes rate limited by diffusion of atomic

oxygen into the remaining metallic core. The logarithmic dependence of the Rh oxidation rate upon time has been reported previously [28], with the rapid formation of an oxide layer decreasing the amount of O<sub>2</sub> dissociation due to self-poisoning.

Analysis of the CO exposure step of the O<sub>2</sub>/CO switching experiment was carried out within the bounds of the signal-to-noise ratio of the EDE data; in general, the RhRh and RhO shells were refined as the single scatterers, and multiple scattering included in Rh–C–O unit, constrained to a coordination number of 1, with a default angle between Rh–C–O being 180°. Upon switching the flowing gas from O<sub>2</sub> to CO at 573 K, an increase of RhRh occupation from ca. 1.3 under O<sub>2</sub> to ca. 4.3 and a reduction of CN<sub>RhO</sub> from ca. 2.6 to ca. 1 are observed under a CO exposure. EXAFS shows the evidence of Rh–CO bonding with the refined angle of the Rh–C–O unit being ~179°. The bond lengths of RhRh, RhO, and Rh–C–O shells are consistent with the crystallographic database. Farrugia reported the crystal structure of Rh<sub>4</sub>(CO)<sub>12</sub> with the mean bond lengths of 2.672 Å for Rh–Rh, 1.951 Å for terminal Rh–C, 2.05 Å for bridged Rh–CO and 3.069 Å for the Rh–C–O distance [29]. Much less disruption of the Rh particles in 4 wt% Rh/Al<sub>2</sub>O<sub>3</sub> over the CO/O<sub>2</sub> cycles is observed at 373 K (Figure S4 and Table S1). Extensive oxidation of Rh particles is indicated by a drop of the RhRh occupation from ca. 5.7 to 2.8 and the presence of a Rh–O shell at 2.01 Å. Upon CO atmosphere the CO adsorption on Rh was also detected in the EXAFS analysis.

Fourier transforms derived from Rh K-edge EDE measurement on 4wt% Rh/Al<sub>2</sub>O<sub>3</sub> during a (O<sub>2</sub>/CO)<sub>3</sub> switching experiment at 573 K (Figure S5) show the gradual decrease of the Rh–Rh coordination number and the evolution of the Rh–O occupation as O<sub>2</sub> is introduced to the catalytic system. The gradual increase of the Rh–Rh occupation and the decrease of Rh–O contribution are observed as the catalyst was exposed to CO. Similar changes are reported in the following O<sub>2</sub>/CO cycles. Clearly, the Rh–Rh contribution increases upon the next CO exposure; however it is still smaller than the Rh–Rh coordination at the beginning of the experiment.

Overall, the combined DRIFTS/XAS studies presented in Figures 3, 4 and 7 indicate a diversity of absorption pathways occurring on the Rh surface under various conditions. In the temperature range of 323–373 K, after an extensive oxidation of Rh particles in the first step, the subsequent CO exposure does not alter the RhRh occupation of Rh catalysts. The DRIFTS results indicate that Rh<sup>I</sup>(CO)<sub>2</sub>, linear and bridged CO species are dominant, with little CO<sub>2</sub> being formed. The following O<sub>2</sub> gas switch oxidises the Rh surface more effectively and promotes the evolution of geminal dicarbonyl species during CO exposures. The IR study over Rh catalysts carried out by Solymosi et al. [30] suggests that the presence of NO (a stronger oxidant than O<sub>2</sub>) assists in the

formation of the geminal dicarbonyl species. It was postulated that NO forms strong bonds with Rh crystallites and causes the oxidative disruption of Rh–Rh bonds to form the Rh(+) sites. The easily dissociable oxidant O<sub>2</sub> also oxidises the Rh nanoparticles. As the temperature rises to 473 K, the same CO species are adsorbed on the Rh surface, however the relative increase of linear CO species can be observed. Consequently, Rh K-edge EXAFS results indicate a growth of Rh particles with temperature under CO atmosphere. In particular, upon subsequent CO exposure at 573 K, an increase of Rh–Rh coordination number is observed from 1.3 to 4.2, corresponding to average particles with ca. 2–4 atoms to 7–10 Rh atoms. Moreover, the presence of Rh–O and Rh–CO neighbouring atoms are detected by EXAFS. In the higher temperature regime (473–573 K), there is a clear synchrony between the O<sub>2</sub>/CO switches and the structural response of the nanoparticulate Rh; mainly the linear CO species forms on metallic fcc Rh under gaseous CO and then Rh is partially oxidised under a flow of O<sub>2</sub>, which is accompanied with CO<sub>2</sub>. The MS data (Figure 5(a)) shows oxidation of adsorbed CO produces less CO<sub>2</sub> than the exposure of oxidised Rh to CO, but does so more rapidly; the more rapid uptake of O<sub>2</sub> by CO covered Rh, as opposed to CO uptake on oxidised Rh was previously reported by Descorme et al. [31] It was shown that the process of CO<sub>2</sub> formation strongly correlates with the oxygen storage on the oxidised catalyst surface when CO molecule is replacing the O atoms. The recent study of CO oxidation reactivity over Rh(111) and Rh(100) by Gustafson et al. shown that the Rh surface is much more active in the surface oxide phase than in the metallic form [32]. On another hand, it was reported that the formation of rhodium oxide leads to catalyst deactivation under highly oxidising conditions (CO:O<sub>2</sub>;1:30) [33].

These results differ from those reported for a 2 wt% Rh/Al<sub>2</sub>O<sub>3</sub> which have been interpreted in terms of a stepwise binding of CO to metallic rhodium, fragmentation of Rh–CO, and then binding of a second CO to the Rh(I) sites in five-coordinate centres [34]. Neither in this study which includes oxygen in the cycle, nor for the direct adsorption of CO [16] do we observe complete fragmentation or obtain any evidence for an isolated Rh–CO centre. Also, periodic DFT calculations suggest that the most stable coordination sites for the Rh<sup>I</sup>(CO)<sub>2</sub> are square-planar, in a variety of surface locations [35].

#### OSM and CSM Rh/CeO<sub>x</sub>/Al<sub>2</sub>O<sub>3</sub>

Ceria was introduced to the Rh catalysts using two preparation methods: (i) OSM of γ-Al<sub>2</sub>O<sub>3</sub> using Ce(acac)<sub>3</sub> and the Rh source added subsequently and, (ii) the CSM technique, by decomposition of Ce(acac)<sub>3</sub> on Rh/γ-Al<sub>2</sub>O<sub>3</sub>. As previously reported [15], the as-synthesised catalysts differ in that the OSM method afforded an increased proportion of Rh<sup>3+</sup> (XPS and

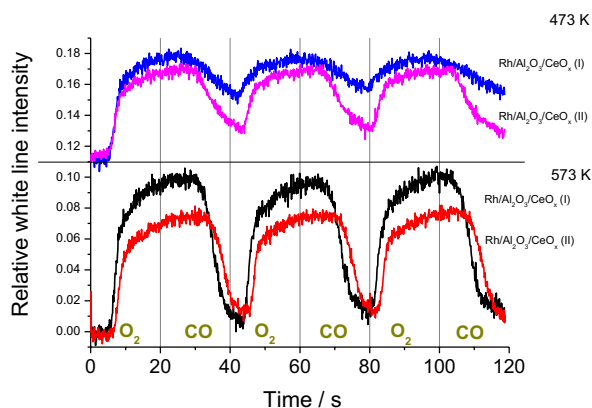


**Figure 8.** Changes in Rh K-edge XANES at 23246 eV during CO oxidation of 4 wt% Rh/CeO<sub>x</sub>/Al<sub>2</sub>O<sub>3</sub> (OSM, I) and 4 wt% Rh/CeO<sub>x</sub>/Al<sub>2</sub>O<sub>3</sub> (CSM, II) at 473 and 573 K. The catalyst was exposed to 5% O<sub>2</sub>/He at the switching times of 0–20 s (I cycle), 40–60 s (II cycle), 80–100 s (III cycle), the flowing gas was switched to CO/He at the switching times of 20–40 s (I cycle), 60–80 s (II cycle) and 100–120 s (III cycle).

XANES) and chlorine content (XPS) as compared to Rh/ $\gamma$ -Al<sub>2</sub>O<sub>3</sub>; the CSM method reduced the Rh<sup>3+</sup> concentration. Figure 8 displays the variation of white line intensity at 23246 eV for 4 wt% Rh/CeO<sub>x</sub>/Al<sub>2</sub>O<sub>3</sub> in the flow of O<sub>2</sub> and CO at 473 and 573 K (Figure S6 shows this data at 323, 373 and 423 K). The variations of white line intensity indicate a relatively simple and progressive increase in a degree of oxidation as a function of temperature. Above 323 K the white line intensity pattern of response to the gaseous environment by the facile oxidation and reduction of the Rh component is repeated throughout the O<sub>2</sub>/CO switches in consistent “cycles”. The overall temporal dependences of the changes in oxidation state observed for both ceriated catalysts are similar to those observed for the non-ceriated Rh sample. However, the magnitude of XANES variation at the selected energy (23246 eV) for 4 wt% CSM Rh/CeO<sub>x</sub>/Al<sub>2</sub>O<sub>3</sub> is smaller than those of OSM ceriated Rh catalysts, and at 573 K less oxidation is observed during the O<sub>2</sub> pulses. These patterns indicate a limitation of the Rh particle oxidation for the sample formed by CSM, wherein some metallic Rh phase is still present under these conditions. Similar structural behaviour of the Rh catalysts was observed in our studies on the Rh catalyst interaction upon CO exposure [16]. It is worth to emphasising that mean Rh particle size of CSM ceriated Rh catalysts is larger as reported by us previously [15], therefore an extensive oxidation of Rh under studied conditions is limited.

The DRIFTS results (Figure S7) demonstrate that all three IR active CO species are formed on the Rh surface of both ceriated Rh catalysts during CO exposure at 323–423 K, as in the case of undoped Rh/Al<sub>2</sub>O<sub>3</sub> sample. The additional broad signal around 1720 cm<sup>−1</sup>, observed only for OSM ceriated Rh/Al<sub>2</sub>O<sub>3</sub>, is characteristic for bridged CO species positioned between Rh and Ce atoms. The same band is observed for CSM Rh/CeO<sub>x</sub>/Al<sub>2</sub>O<sub>3</sub> at ca. 1650 cm<sup>−1</sup> (323 K) and at ca. 1666 cm<sup>−1</sup> (573 K). This

characteristic peak of CO band at 1725 cm<sup>−1</sup> is consistent with previously observed band by Kiennemann et al. in the IR study of CO interactions with Rh/CeO<sub>2</sub>/SiO<sub>2</sub> [36]. It is worthy of mentioning that a silica surface has higher surface charges than alumina due to its more electropositive covalence, therefore it would be expected that bridged CO species between Rh and Ce atoms will be present at lower frequency for alumina supported catalysts. However, the intensity of the formed species increased in succeeding O<sub>2</sub>/CO cycles at the expense of linear CO species. Moreover, if there would be any direct Ce–CO<sub>x</sub> species detected by IR, the bidentate carbonate species, [Ce(O)<sub>2</sub>CO], with a characteristic frequency at ca. 1562 cm<sup>−1</sup> would be the most common such form. This was not observed, and no other direct “Ce–CO<sub>x</sub>” species could identified in catalysts studied.

Furthermore, a new band is detected at 2134 and 2139 cm<sup>−1</sup> for both samples at 423 K. In the light of previous findings, the peak position of these species (>2134 cm<sup>−1</sup>) is rather controversial. Others have observed the band at 2177 cm<sup>−1</sup> assigned to CO linearly adsorbed on Ce<sup>4+</sup> and the signal at 2156 cm<sup>−1</sup> to Ce<sup>4+</sup> in a more unsaturated coordination state [37]. That would suggest that the signal at ca. 2134 cm<sup>−1</sup> is attributed to RhO(CO) species, shifted from 2125 cm<sup>−1</sup> for undoped Rh catalyst to 2134–2139 cm<sup>−1</sup> for ceriated Rh materials; by virtue for its energy and behaviour [38]. The shift to higher frequency of RhO(CO) species for ceriated samples is consistent with the results of CO adsorption without O<sub>2</sub> gas [16] wherein the high frequency shift for the linear CO species was attributed to a strong Ce–Rh interaction which reduces the electron density used for back bonding and consequently weakens the Rh–CO bond, as in the Blyholder model [39]. This spectroscopic feature correlates well with the kinetic results that show a significant decrease in the adsorption enthalpy of CO on Pt/Rh/Al<sub>2</sub>O<sub>3</sub>/CeO<sub>2</sub> when compared to the non-ceriated Rh catalysts [40]. The integrated intensities of the adsorption bands for linear CO species are relatively higher for the CSM ceriated Rh catalyst.

When increasing the temperature to 573 K, a shift for the linear species from 2074 to 2045 cm<sup>−1</sup> was observed as well as increase in the energy of the stretching mode for the bridged species: from 1867 to 1908 cm<sup>−1</sup> for OSM Rh/CeO<sub>x</sub>/Al<sub>2</sub>O<sub>3</sub>. Similar trends for the band shifts are detected for Rh catalysts ceriated by CSM; the frequencies of the linear, bridged CO and RhO(CO) species were shifted to higher frequency at each temperature compared to OSM ceriated Rh catalysts. It is noteworthy that no RhO(CO) were detected for the CSM ceriated Rh catalyst at 573 K, unlike the undoped and OSM catalyst; this indicates the absence of Rh oxidation under CO exposure for this catalyst. The observed IR results for ceriated Rh catalysts, when compared to undoped Rh material, suggest again a close proximity between Rh and CeO<sub>x</sub> molecules specifically for CSM Rh/CeO<sub>x</sub>/

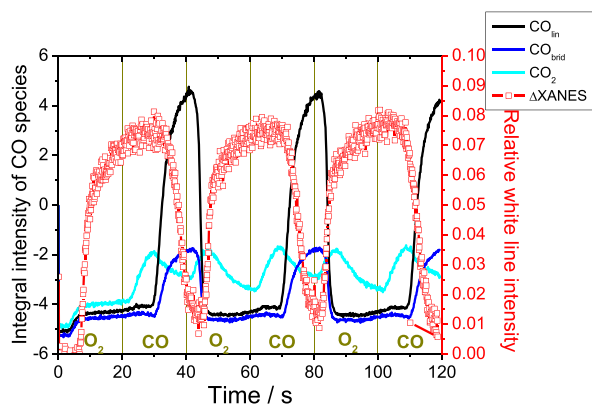


**Figure 9.** Variation of integral intensity of CO species and  $\Delta$ XANES differences in white line intensity at 23246 eV during the  $O_2$ /CO switching experiment over CSM 4 wt% Rh/CeO<sub>x</sub>/Al<sub>2</sub>O<sub>3</sub> at 573 K. The catalyst was exposed to 5%  $O_2$ /He at the switching times of 0–20 s (I cycle), 40–60 s (II cycle), 80–100 s (III cycle), the flowing gas was switched to CO/He at the switching times of 20–40 s (I cycle), 60–80 s (II cycle) and 100–120 s (III cycle).

Al<sub>2</sub>O<sub>3</sub>, where CeO<sub>x</sub> effectively protects Rh particles from extensive oxidation.

Figure 9 combines the two experimental techniques by indexing the variation of white line intensity at 23250 eV and the DRIFTS integrals of the two dominant surface CO species (linear, bridged) throughout  $O_2$ /CO switching experiment over CSM Rh/CeO<sub>x</sub>/Al<sub>2</sub>O<sub>3</sub> at 573 K. Firstly, an initial switch to  $O_2$  atmosphere induces a rapid Rh oxidation that is stabilised after 15 s and, when switching the flowing gas to CO, CO<sub>2</sub> gas is produced and with delayed reduction of the Rh. The variations of the Rh structure are mirrored by the IR results with a sharp increase in integral intensity for both IR active species (linear and bridged). The constant “cycles” can be viewed to proceed with the gas switching: the evolution/depopulation of CO species with the oscillation of the Rh oxidation. Moreover, the doping of ceria to Rh catalysts induces the evolution of CO species to be more constant throughout the entire experiment as compared with the undoped Rh/Al<sub>2</sub>O<sub>3</sub> sample.

Rh K-edge EXAFS analysis was carried out for the ceriated Rh catalysts also using the same modelling procedure as for Rh/Al<sub>2</sub>O<sub>3</sub>. No Rh–Ce or Rh–O–Ce paths were detected throughout the entire process of CO oxidation or under calcinations/reduction conditions. Miyazawa et al. [41] reported *in situ* QEXAFS studies on Rh/CeO<sub>2</sub>/SiO<sub>2</sub> wherein a formation of the Rh–O–Ce bond was detected in the oxidation/reduction processes, but these were not evident in with the short acquisition times in our study. The temporal variations of Rh–Rh coordination number of the two ceriated Rh catalysts upon  $O_2$ /CO cycles are shown in Figure 10. The structural parameters refined in the EXAFS data analysis are enclosed in Table S2 and S3 in the Supporting Information. It is evident that the Rh–Rh occupation is larger for CSM Rh catalyst at an initial step of the reaction (when reduced), when compared to OSM Rh

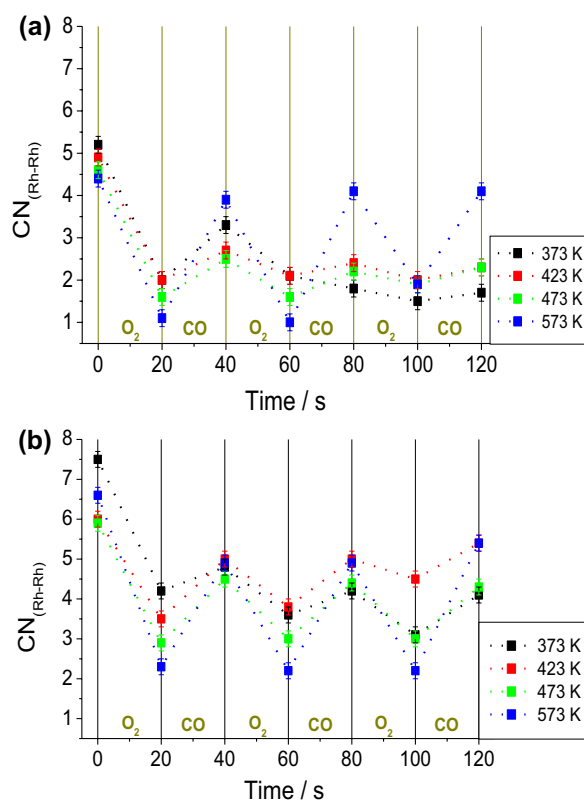


**Figure 10.** Variations of RhRh coordination number during the  $O_2$ /CO switching experiment over (a) OSM 4 wt% Rh/CeO<sub>x</sub>/Al<sub>2</sub>O<sub>3</sub> and (b) CSM 4 wt% Rh/CeO<sub>x</sub>/Al<sub>2</sub>O<sub>3</sub> at the temperatures investigated. The catalyst was exposed to 5%  $O_2$ /He at the switching times of 0–20 s (I cycle), 40–60 s (II cycle), 80–100 s (III cycle), the flowing gas was switched to CO/He at the switching times of 20–40 s (I cycle), 60–80 s (II cycle) and 100–120 s (III cycle).

sample, that directly corresponds to larger Rh particle size present throughout the whole CO oxidation process. In general, the variations in Rh–Rh occupation that do occur for CSM Rh catalyst in studied temperature range and for OSM Rh catalyst at 573 K appear to follow the gas switching such as a decrease of  $CN_{RhRh}$  during  $O_2$  exposure and an increase of Rh occupation while CO exposure indicating clear oscillations of structural changes. For OSM Rh/CeO<sub>x</sub>/Al<sub>2</sub>O<sub>3</sub> at 373 K there is a drift to lower RhRh coordination numbers consistent with the IR indications of an increase in Rh<sup>I</sup>(CO)<sub>2</sub>, whilst at 423 and 473 K there is no significant change in the Rh–Rh coordination following the initial, extensive oxidation (large drop of  $CN_{RhRh}$ ). A significant increase in the mean RhRh shell coordination number of CSM ceriated Rh catalyst ( $CN_{RhRh} \sim 6.6$  upon  $H_2$  at 573 K) compared to that for OSM Rh/CeO<sub>x</sub>/Al<sub>2</sub>O<sub>3</sub> ( $CN_{RhRh} \sim 4.5$  upon  $H_2$  at 573 K), implies a greater mean particle size throughout the entire experiment. The EXAFS data suggests that similar or higher level of the Rh disruption occurred on the Rh surface of the OSM ceriated Rh catalyst as for undoped Rh/Al<sub>2</sub>O<sub>3</sub> catalysts across all the temperatures studied. These results would suggest that OSM Rh/CeO<sub>x</sub>/Al<sub>2</sub>O<sub>3</sub> may lower the Rh–Rh coordination indicating lower mean Rh particles under conditions studied.

In summary, the EDE/DRIFTS/MS results presented for 4 wt% OSM Rh/CeO<sub>x</sub>/Al<sub>2</sub>O<sub>3</sub> and elemental 4 wt% Rh/Al<sub>2</sub>O<sub>3</sub> catalysts indicate both systems have similar behaviour in terms of selectivity, metal phase changes and activity during CO oxidation. In the lower temperature regime (323–423 K), the Rh component was oxidised in a similar way to an undoped sample. However, at 473 K, the Rh particles are even more oxidised than for the unciliated sample. On another hand, significant differences of catalytic and structural behaviour are observed between the two catalysts: Rh/Al<sub>2</sub>O<sub>3</sub> and CSM Rh/CeO<sub>x</sub>/Al<sub>2</sub>O<sub>3</sub>, produced by doping of ceria to pre-supported Rh on alumina. At the start of the experiment larger Rh particles are present in the ciliated Rh catalyst e.g. at 573 K an average Rh particle is composed of ca. 24–33 Rh atoms and for undoped Rh catalyst it is ca. 13–19 atoms. Based on the EDE/DRIFTS/MS data on CSM ciliated Rh catalyst we can confirm a presence of larger Rh particles and a close proximity between Rh and CeO<sub>x</sub> molecules which influences a structural behaviour of this catalyst upon CO oxidation.

## Conclusion

In situ, time-resolved EDE/DRIFTS/MS studies on Rh/Al<sub>2</sub>O<sub>3</sub> and Rh/Al<sub>2</sub>O<sub>3</sub> doped by ceria during the process of CO oxidation revealed very rapid and reversible structural changes of the catalyst and its reactivity. Introducing O<sub>2</sub> to reduced Rh particles that undergo rapid and extensive oxidation, subsequent flowing CO reduces the oxide and leaves the system in a more metallic phase. While the IR results indicate that mostly geminal dicarbonyl species, linear and bridged CO species adsorbed on the Rh surface after CO exposure below 473 K, however at 573 K mainly the linear and bridged CO species are formed on the Rh surface, suggesting the formation of the metallic Rh phase under these conditions even though the Rh catalysts were previously oxidised. The degree of Rh oxidation as well as the variations of the Rh–Rh coordination number throughout O<sub>2</sub>/CO cycles increases with temperature. Although it was not possible to identify the structural reasons for the oscillations in catalytic activity, the reactions of terminal and bridging CO with O<sub>2</sub> to form CO<sub>2</sub> and oxidise the rhodium is evident, as is the reverse reduction of oxidised rhodium to the metal and concomitant evolution of CO<sub>2</sub>. With a mean Rh–Rh coordination number of 5.7(2), the mean particle size of rhodium is very small, and the majority are oxidised under O<sub>2</sub>. The pulsed experiments indicate that the Rh particles store ~1 CO/Rh and 2O/Rh when the environment is rich in those gases.

Even with this low ratio of ceria to rhodium (1:1), the proximity of the metals results in observable changes in behaviour. Interestingly the apparent particle size of the rhodium increases for the Ce promoter through the sequence of O<sub>2</sub>/CO cycles, suggesting a slower equilibration. The similarity in the quantities of adsorbed CO

that is oxidised by each of the catalysts during an O<sub>2</sub> pulse suggests that the heterometals, which stabilise the Rh particles against oxidation, are covering little or no rhodium surface. Their influence though does indicate a close proximity that can increase the sequestering of available oxygen. The implication of the Rh XAFS results is that the storage of this oxygen is associated with the heterometals rather than rhodium.

## Experimental section

### Sample preparation

**Rh/γ-Al<sub>2</sub>O<sub>3</sub>:** 4 wt% Rh/γ-Al<sub>2</sub>O<sub>3</sub> supported samples were prepared through wet impregnation of Al<sub>2</sub>O<sub>3</sub> (Degussa, Alumina C, surface area ca. 88 m<sup>2</sup> g<sup>-1</sup>; 1.92 g) with RhCl<sub>3</sub>·3H<sub>2</sub>O (0.21 g) in aqueous solution. This was stirred, using a Teflon-coated magnetic stirrer until a uniform paste was achieved. The sample was then dried in air. Subsequently the resultant was calcined for 6 h at 673 K in 5% O<sub>2</sub>/He and reduced for 5 h under flowing 5% H<sub>2</sub>/He at 573 K.

**OSM ciliated Rh/γ-Al<sub>2</sub>O<sub>3</sub>:** 5 wt% Ce/γ-Al<sub>2</sub>O<sub>3</sub> support was produced by dissolving cerium (III) 2,4-pentanedionate (0.509 g) in toluene and of γ-Al<sub>2</sub>O<sub>3</sub> (1.805 g) added. The sample was dried overnight in the air before being calcined under 5% O<sub>2</sub>/He for 6 h at 773 K. Subsequently the solution of RhCl<sub>3</sub>·H<sub>2</sub>O in water was added to a suspension of Al<sub>2</sub>O<sub>3</sub>/CeO<sub>2</sub> support and stirred. The sample was then dried overnight in air before being calcined under 5% O<sub>2</sub>/He for 6 h at 773 K and reduced under 5% H<sub>2</sub>/He for 5 h at 300 °C.

**CSM ciliated, Ce/ Rh/γ-Al<sub>2</sub>O<sub>3</sub>:** Rh/γ-Al<sub>2</sub>O<sub>3</sub>, (1 g) was re-reduced under flowing 5% H<sub>2</sub>/He for 3 h at 573 K. To prepare 5 wt% Ce of Rh catalysts, a solution of Ce(acac)<sub>3</sub> (0.164 g) in toluene (100 ml) was placed in the three-way tap dropper, purged by N<sub>2</sub> for 15 min and added drop wise to the reduced catalyst. Subsequently, the reagents were mixed under flowing 5% H<sub>2</sub>/He at 353 K for 8 h. Then, the sample was filtered and dried in air overnight. The sample was again reduced under 5% H<sub>2</sub>/He at 573 K for 3 h. All preparations were performed under N<sub>2</sub> atmosphere.

**Sample pre-treatment:** Prior to the measurement all the samples have been reduced *in situ* (in the DRIFTS cell) for the XAFS measurements. These samples are denoted “reduced”. The *in situ* reduction is performed as followed: Reduction in 5% H<sub>2</sub>/He up to 573 K; oxidation under 5% O<sub>2</sub>/He at 573 K until remaining carbonaceous deposits have been removed from the catalyst (by observing carbon related fragments in the MS); at 573 K back to 5% H<sub>2</sub>/He; cooling down to room temperature in 5% H<sub>2</sub>/He.

**Energy dispersive X-ray absorption spectroscopy (EDE):** Rh K-edge XAFS spectra were measured in transmission using a Si (3 1 1) polychromator mounted in a Bragg configuration. The EDE measurement was

performed at the European Synchrotron Radiation Facility (ESRF) in Grenoble, France at ID24. EXAFS detection was done via the FReLoN CCD camera with a total acquisition time with 10 spectra of ca. 10 ms. The DRIFTS measurement was performed simultaneously, with the same sampling rates for each spectroscopy whilst a mass spectrometer continuously measured the composition of the gas phase.

**DRIFTS:** The infrared measurements were performed using Bruker IFS 66/S spectrometer equipped with a narrow band, linearised, MCT detector with 4 cm<sup>-1</sup> resolution. Acquisition time for a single spectrum was ca. 100 ms. The total catalyst load in the DRIFTS sample bed was about 0.025 g.

**O<sub>2</sub>/CO switching experiment:** O<sub>2</sub>/CO gas switching studies were performed by combined EDE/DRIFTS/MS apparatus at ID24 [16]. The switching experiment was done at selected temperatures: 323, 373, 423, 473 and 573 K. The order of gases was as follow: He-O<sub>2</sub> > CO > O<sub>2</sub> > CO > O<sub>2</sub> > CO-He with a gas flow of 25 mlmin<sup>-1</sup>. The total catalyst load was ca. 0.025 g.

**Data handling and analysis:** The EDE calibration was carried out using XOP programme [42] by comparing an EDE foil spectrum to an EXAFS foil spectrum and correcting the offset of the edge jump and multiplying the pixel number by a factor to obtain the energies. From the calibrated EDE foil the offset and multiplication factor parameters were used to calibrate of the EDE spectra collected. Data reduction was carried out using Xmult [43] and analysis was made using a spherical wave formalism using EXCURV98 [44] “R factors” quoted are defined as  $R = (\int [\chi T - \chi E] k n dk / [\chi E] k n dk) 100\%$  where  $\chi T$  and  $\chi E$  are the theoretical and experimental EXAFS,  $k$  is the photoelectron wave vector,  $dk$  is the range of photoelectron wave vectors analysed, and  $n$  is the weighting in  $k$  applied to the data. The number of parameters,  $N$ , that can be justifiably fit was estimated from the Nyqvist equation:  $N = (2\Delta k \Delta r / \pi) + 1$  where  $\Delta k$  and  $\Delta r$  are the ranges in  $k$ - and  $r$ -space over which the data are analysed. DW factors for Rh-Rh and Rh-O shells were estimated for Rh/Al<sub>2</sub>O<sub>3</sub> and subsequently the spectra for the whole range of Rh catalysts were analysed in the same  $k$  range holding DW factor constant ( $2\sigma^2 = 0.012\sigma^2$ ). The C-O contribution directly bonded to Rh was defined as a unit applying multiple scattering. As presented by Binsted et al. [45], the spherical wave theory with multiple scattering was used to refine the structural parameters for carbonyl groups and to estimate the Rh-C-O bond angle. Error in coordination number should be considered in the range  $\pm 10$ –20%, errors in bond length determination are estimated at about 2%. Ef for each refinement was within the energy range of (–5) to 5 eV.

## Acknowledgements

We wish to thank the ESRF for access to facilities and to the ESRF (CH-2125, CH-2194, CH-2452, CH-2553) and EPSRC

for funding this research and a post doctoral position (GR/S85818/01) and EPSRC Advanced Research Fellowship (EP/E060404/1) (both to M.T.) and a studentship to A.B.K. (ESRF and EPSRC).

## Disclosure statement

No potential conflict of interest was reported by the authors.

## Funding

This work was supported by Engineering and Physical Sciences Research Council (EPSRC) [GR/S85818/01], [EP/E060404/1].

## ORCID

John Evans  <http://orcid.org/0000-0003-3290-7785>

## References

- [1] Anderson JA. CO oxidation on Rh/Al<sub>2</sub>O<sub>3</sub> catalysts. *J Chem Soc Faraday Trans.* **1991**;87:3907–3911.
- [2] Cavers M, Davidson JM, Harkness IR, et al. Spectroscopic identification of the active site for CO oxidation on Rh/Al<sub>2</sub>O<sub>3</sub> by concentration modulation *in situ* DRIFTS spectroscopic identification of the active site for CO oxidation on Rh/Al<sub>2</sub>O<sub>3</sub> by concentration modulation *in situ* DRIFTS. *J Catal.* **1999**;188:426–430.
- [3] Ioannides T, Efstathiou AM, Zhang ZL, et al. CO oxidation over Rh dispersed on SiO<sub>2</sub>, Al<sub>2</sub>O<sub>3</sub>, and TiO<sub>2</sub>: kinetic study and oscillatory behavior. *J Catal.* **1995**;156:265–272.
- [4] Newton MA, Dent AJ, Diaz-Moreno S, et al. Rapid monitoring of the nature and interconversion of supported catalyst phases and of their influence upon performance: CO oxidation to CO<sub>2</sub> by  $\gamma$ -Al<sub>2</sub>O<sub>3</sub> supported Rh catalysts. *Chem Eur J.* **2006**;12:1975–1985.
- [5] Oh SH, Fisher GB, Carpenter JE, et al. Comparative kinetic studies of CO–O<sub>2</sub> and CO–NO reactions over single crystal and supported rhodium catalysts. *J Catal.* **1986**;100:360–376.
- [6] Oh SH, Eickel CC. Influence of metal particle size and support on the catalytic properties of supported rhodium: CO–O<sub>2</sub> and CO–NO reactions. *J Catal.* **1991**;128:526–536.
- [7] Gandhi HS, Graham GW, McCabe RW. Automotive exhaust catalysis. *J Catal.* **2003**;216:433–442.
- [8] Kummer JT. Use of noble metals in automobile exhaust catalysts. *J Phys Chem.* **1986**;90:4747–4752.
- [9] Twigg MV. Roles of catalytic oxidation in control of vehicle exhaust emissions. *Catal Today.* **2006**;117:407–418.
- [10] Armor JN. Review: the multiple roles for catalysis in the production of H<sub>2</sub>. *App Catal A.* **1999**;176:159–176.
- [11] Rostrup-Nielsen JR. Catalysis steam reforming. In: Anderson JR, Boudart M, editors. *Catalysis: science & technology*. Vol. 5. Berlin: Springer; **1984**. 1–117.
- [12] Oh SH, Eickel CC. Effects of cerium addition on CO oxidation kinetics over alumina supported rhodium catalysts. *J Catal.* **1988**;112:543–555.
- [13] Polvinen R, Vippola M, Valden M, et al. The effect of Pt–Rh synergism on the thermal stability of rhodium oxide on pure alumina and Ce–ZrO<sub>2</sub>-modified alumina-supported catalysts. *J Catal.* **2004**;226:372–381.

- [14] Yao YFY. The oxidation of CO and hydrocarbons over noble metal catalysts. *J Catal.* **1984**;87:152–162.
- [15] Kroner AB, Newton MA, Tromp M, et al. Structural characterization of alumina-supported Rh catalysts: effects of ceriation and zirconiation by using metal–organic precursors. *ChemPhysChem.* **2013**;14:3606–3617.
- [16] Kroner AB, Newton MA, Tromp M, et al. Time-resolved, *in situ* DRIFTS/EDE/MS studies on alumina-supported rhodium catalysts: effects of ceriation and zirconiation on rhodium–CO interactions. *ChemPhysChem.* **2014**;15:3049–3059.
- [17] Rice CA, Worley SD, Curtis CW, et al. The oxidation state of dispersed Rh on Al<sub>2</sub>O<sub>3</sub>. *J Chem Phys.* **1981**;74:6487–6497.
- [18] Primet M. Infrared study of CO chemisorption of zeolite and alumina supported rhodium. *J Chem Soc Faraday Trans I.* **1978**;74:2570–2580.
- [19] Yang AC, Garland CW. Infrared studies of carbon monoxide chemisorbed on rhodium. *J Phys Chem.* **1957**;61:1504–1512.
- [20] Yates JT, Duncan TM, Vaughan RW. Infrared spectroscopic study of activated surface processes: CO chemisorption on supported Rh. *J Chem Phys.* **1979**;71:3908–3915.
- [21] Laachir A, Perrichon V, Badri A, et al. Reduction of CeO<sub>2</sub> by hydrogen magnetic susceptibility and Fourier-transform infrared, ultraviolet and X-ray photoelectron spectroscopy measurements. *J Chem Soc Faraday Trans.* **1991**;87:1601–1609.
- [22] Sugiura M. Oxygen storage materials for automotive catalysts: ceria-zirconia solid solutions. *Catal Surv Asia.* **2003**;7:77–87.
- [23] Jentys A. Estimation of mean size and shape of small metal particles by EXAFS. *Phys Chem Chem Phys.* **1999**;1:4059–4063.
- [24] Martens JHA, Prins R, Zandbergen H, et al. Structure of Rh/TiO<sub>2</sub> in the normal and SMSI state as determined by EXAFS and HRTEM. *J Phys Chem.* **1988**;92:1903–1916.
- [25] Martens JHA, Prins R, Koningsberger DC. Controlled oxygen chemisorption on an alumina supported rhodium catalyst. The formation of a new metal-metal oxide interface determined with EXAFS. *J Phys Chem.* **1989**;93:3179–3185.
- [26] Gustafson J, Mikkelsen A, Borg M, et al. Self-limited growth of a thin oxide layer on Rh(111). *Phys Rev Lett.* **2004**;92:126102-1–4.
- [27] Gustafson J, Mikkelsen A, Borg M, et al. Structure of a thin oxide film on Rh(100). *Phys Rev B.* **2005**;71:115442-1–9.
- [28] Newton MA, Fiddy SG, Guilera G, et al. Oxidation/reduction kinetics of supported Rh/Rh<sub>2</sub>O<sub>3</sub> nanoparticles in plug flow conditions using dispersive EXAFS. *Chem Commun.* **2005**;1:118–120.
- [29] Farrugia LJ. Structural redetermination of Rh<sub>4</sub>(CO)<sub>12</sub> at 293 and 173 K and analysis of the thermal motion in relation to the dynamical behavior. *J Cluster Sci.* **2000**;11:39–53.
- [30] Solymosi F, Bansagi T, Novak E. Effect of NO on the CO-induced disruption of rhodium crystallites. *J Catal.* **1988**;112:183–193.
- [31] Descorme C, Taha R, Mouaddib-Moral N, et al. Oxygen storage capacity measurements of three-way catalysts under transient conditions. *App Catal A.* **2002**;223:287–299.
- [32] Gustafson J, Westerström R, Mikkelsen A, et al. Sensitivity of catalysis to surface structure: The example of CO oxidation on Rh under realistic conditions. *Phys Rev B.* **2008**;78:045423-1–6.
- [33] Kellogg GL. The oxidation of rhodium Field-Emitter surfaces during the CO oxidation reaction. *J Catal.* **1985**;92:167–172.
- [34] Suzuki A, Inada Y, Yamaguchi A, et al. Time scale and elementary steps of CO-induced disintegration of surface rhodium clusters. *Angew Chem.* **2003**;115:4943–4947; *Angew Chem Int Ed.* **2003**;42:4795–4799.
- [35] Roscioni OM, Dyke JM, Evans J. Structural characterisation of supported Rh(CO)<sub>2</sub>/γ-Al<sub>2</sub>O<sub>3</sub> catalysts by periodic DFT calculations. *J Phys Chem C.* **2013**;117:19646–19470.
- [36] Kiennemann A, Breault R, Hindermann J-P, et al. Ethanol promotion by the addition of cerium to rhodium-silica catalysis. *J Chem Soc Faraday I.* **1987**;83:2119–2128.
- [37] Li C, Sakata Y, Arai T, et al. Carbon monoxide and carbon dioxide adsorption on cerium oxide studied by Fourier-transform infrared spectroscopy. Part 1—Formation of carbonate species on dehydroxylated CeO<sub>2</sub> at room temperature. *J Chem Soc.* **1989**;85:929–943.
- [38] Binet C, Badri A, Lavalley J-C. A spectroscopic characterization of the reduction of ceria from electronic transitions of intrinsic point defects. *J Phys Chem.* **1994**;98:6392–6398.
- [39] Blyholder G. Molecular orbital view of chemisorbed carbon monoxide. *J Phys Chem.* **1964**;68:2772–2777.
- [40] Granger P, Delannoy L, Lecomte JJ, et al. Kinetics of the CO+NO reaction over bimetallic platinum–rhodium on alumina: effect of ceria incorporation into noble metals. *J Catal.* **2002**;207:202–212.
- [41] Miyazawa T, Okumara K, Kunimori K, et al. Promotion of oxidation and reduction of Rh species by interaction of Rh and CeO<sub>2</sub> over Rh/CeO<sub>2</sub>/SiO<sub>2</sub>. *J Phys Chem C.* **2008**;112:2574–2583.
- [42] Sanchez del Rio M. Xop/Xplot user's guide. Grenoble: ESRF; **2001**.
- [43] Binsted N. X-Mult. Southampton: University of Southampton; **2006**.
- [44] Binsted N. EXCURV(9.301). Daresbury: CCLRC Daresbury Laboratory computer program; **1998**.
- [45] Binsted N, Cook SL, Evans J, et al. EXAFS and near-edge structure in the cobalt K-edge absorption spectra of metal carbonyl complexes. *J Am Chem Soc.* **1987**;109:3669–3676.